Synthesis of Mesostructured Iron Oxides with Potential As(V) Adsorption Application

LI Fei-hu[1*], FU Xiao-ru[1], HUANG Jie[1] and ZHAI Jian-ping[2]

1. Jiangsu Provincial Key Laboratory of Atmospheric Environment Monitoring and Pollution Control, School of Environmental Science and Engineering, Nanjing University of Information Science and Technology, Nanjing 210044, P. R. China;

2. State Key Laboratory of Pollution Control and Resource Reuse, School of Environment, Nanjing University, Nanjing 210046, P. R. China

Abstract Mesostructured iron oxides(MIOs) were nanocasted from a plugged hexagonal templated silica(PHTS) with a Brunauer-Emmett-Teller(BET) surface area of 694 m^2/g. Results of X-ray diffraction(XRD), transmission electron microscopy(TEM) and N_2 adsorption-desorption suggest that the nanocasted MIOs are synthetic hematite(α-Fe_2O_3) with a wormhole-like mesoporous network. As(V) adsorption test shows that the selected MIO——MIO-500(calcinated at 500 °C) with a BET surface area of 82 m^2/g has a maximum adsorption capacity of 5.39 mg/g for As(V), which is 2.5 times as large as that of natural hematite adsorbent. The study suggests that MIOs could be potentially used as the adsorbent of As(V) in wastewater.

Keywords Mesostructured iron oxide; Plugged hexagonal templated silica(PHTS); Nanocasting; Arsenate; Adsorption

Article ID 1005-9040(2012)-04-559-04

1 Introduction

Mesostructured metal oxides have the immense potential of application in adsorption, catalysis, photocatalysis, sensors and electrode materials because of their characteristic complexing, catalytic, optical and electronic properties[1—5]. There have been many strategies reported for preparing mesostructured metal oxides including surfactant-templating(also called soft-templating), nanocasting(also called hard-templating), nanocrystal templating, etc.[2]. As for mesostructured iron oxides(MIOs), Huo *et al*.[6] made first attempt to prepare MIOs with lamellar phase *via* an anionic surfactant-templating approach. Using non-ionic surfactant-templating method, Yang *et al*.[1] prepared a variety of mesostructured metal oxides but Fe_2O_3. Jiao *et al*.[7] reported well-defined MIOs using decylamine as template. Han *et al*.[8] also synthesized mesoporous Fe_2O_3 microspheres *via* a polymerization-induced colloid aggregation strategy. Our previous work[9] demonstrated the synthesis of mesostructured ferric oxyhydroxides *via* an alkyl surfactant-templating approach as well.

As a novel concept and approach, nanocasting was firstly adopted in the syntheses of mesoporous carbon[10—12] and metal oxides[13—15]. The pore features of nanocasted materials depend greatly upon the parent hard-templates. For example, KIT-6 with 3D pore connection is capable of nanocasting ordered MIOs with connected mesopores[16,17], whereas SBA-15 with 2D channels can only generate Fe_2O_3 nanowire[18]. Recently, a plugged hexagonal templated silica(PHTS) with micro- and mesopores and internal silica nanocapsules has been reported[19]. This novel PHTS is interesting and may be suitable for nanocasting MIOs with joint mesopores.

Herein we present a simple one-pot procedure to fabricate PHTS. Using the PHTS as a hard-template, we nanocasted MIOs with connected wormhole-like mesopores. The MIOs showed a better performance in adsorption of As(V) from aqueous solution compared with natural hematite(α-Fe_2O_3) adsorbents.

2 Experimental

2.1 Synthesis of PHTS and MIOs

All the chemicals were purchased from Sinopharm Chemical Reagent Co., Ltd., China, and used as received. PHTS was hydrothermally synthesized according to the literature method[19,20] with minor changes. Typically, 8.54 g of P123 was dissolved in a solution of HCl(52.55 g, 37%, mass fraction) in water(260 g) and stirred at 40 °C until a homogeneous solution was achieved. Then 20 g of technical-grade sodium silicate solution/water glass(11.3% Na_2O, 26.7% SiO_2, mass fraction) was added to the solution that was sealed up and stirred at 40 °C for 20 h, followed by static ageing at 80 °C for 24 h. The resultant product was recovered, washed with anhydrous alcohol at least three times, dried in an oven at 150 °C for 6 h, and finally heated to 550 °C for 6 h. For comparison, SBA-15 was

*Corresponding author. E-mail: favorlee@163.com

Received October 10, 2011; accepted May 14, 2012.

Supported by the National Natural Science Foundation of China(No.51002080), the Research Funds of Nanjing University of Information Science and Technology(NUIST), China(No.S8108179001), the College Students Practice Innovative Projects of Jiangsu Province, China(No.N1885010087) and the Priority Academic Program Development of Jiangsu Higher Education Institutions, China.

also prepared in terms of Zhao *et al.*'s procedure[20].

MIOs were prepared according to the typical nanocasting procedure[16]. Based on different calcinating temperatures, MIOs samples calcinated at 500 and 600 °C were termed as MIO-500 and MIO-600, respectively.

2.2 Characterization

The XRD patterns of PHTS and the nanocasted MIOs were recorded on an ARL X'TRA X-ray diffractmeter(Cu *Kα* radiation). Transmission electron microscopy(TEM, JEOL JEM-200CX, 200 kV) analysis was employed to clarify the detailed structural ordering of such materials. The detailed pore structures of PHTS and MIOs were examined by N_2 adsorption-desorption(Micromeritics ASAP 2010).

2.3 Adsorption Test of As(V)

MIO heated at 500 °C, *i.e.*, MIO-500, and a certain natural hematite(α-Fe_2O_3) adsorbent(purchased from Nanjing Wanqing Chemistry Co., Ltd., China) were selected as adsorbents for As(V) in aqueous solution. In a typical adsorption test, 100 mg of adsorbent was added separately to a conical flask(250 mL) before 100 mL of As(V) solution with given concentration, pH(7.0±0.1) and ionic strength(I=0.01 mol/L NaCl) was added. Having been sealed and premixed on a vortex mixer for 5 min, the mixture was shaken at 180 r/min and 25 °C for approximate 24 h on a reciprocal shaker. Then, it was filtered with a 45 μm membrane filter for analysis. The pH was measured with a pH meter(model 828, Orion, US). As(V) in the supernatant was analyzed on an AFS-610 atomic fluorescence spectrometer (Beijing Rayleigh Analytical Instrument Co., China) *via* the hydride-generation atomic fluorescence spectrometry(HG-AFS) procedure. The adsorption isotherms were studied by varying the concentration of As(V) solution with a fixed dose of adsorbent(*i.e.*, 100 mg). Adsorption isotherms were fitted *via* both Langmuir and Freundlich equations as depicted in our previous publication[9].

3 Results and Discussion

As shown in Fig.1, the PHTS exhibits nearly the same X-ray diffraction(XRD) pattern as SBA-15, a typical XRD pattern of mesoporous materials with 2D hexagonal space group *P6mm*[20], indicating that PHTS has a similar mesostructure as SBA-15. The diffraction peak at 2θ=0.428°, corresponding to a d spacing of 10.3 nm(Cu *Kα*, λ=0.15405 nm), may be indexed as the (100) reflection. The (100) reflection gives a unit cell parameter a_0 of 11.89 nm as calculated with the equation $a_0=2d_{(100)}/\sqrt{3}$[20].

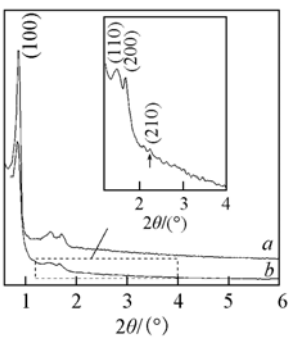

Fig. 1 XRD patterns of SBA-15(*a*) and PHTS(*b*)

TEM images of SBA-15 and PHTS(Fig.2) show that PHTS has a large-scale well-ordered 2D hexagonal array of mesopores, similar to those typically observed for SBA-15[20], implying that they have similar mesostructures verified by XRD analysis.

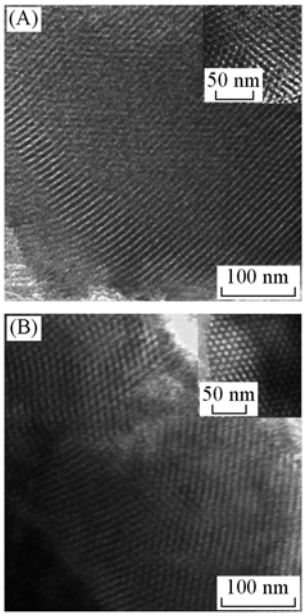

Fig.2 TEM images of SBA-15(A) and PHTS(B) along [100] direction and along [110] direction (insets)

The N_2 adsorption-desorption isotherms and pore size distribution curves of SBA-15 and PHTS are shown in Fig.3. Both isotherms are featured by type IV isotherm with type H2

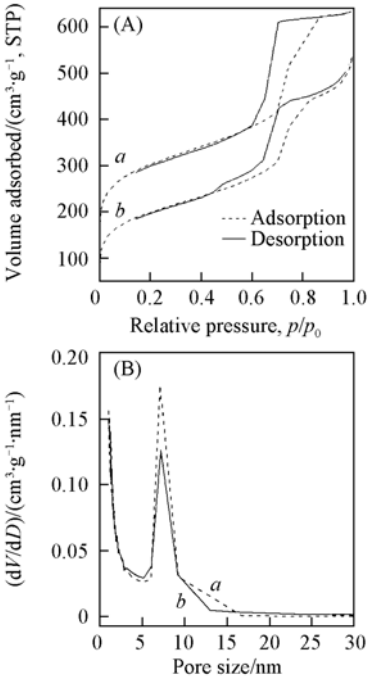

Fig.3 N_2 adsorption-desorption isotherms(A) and pore size distribution curves(B) of SBA-15(*a*), and PHTS(*b*)

uniform channels-like mesopores in both materials[21]. It is, however, interesting to note that the desorption isotherm of PHTS has three steps, *i.e.* the p/p_0 ranges of 1.0—0.6, 0.6—0.4 and 0.4—0, respectively. This observation is an evidence of the existence of plugged mesopores in hexagonal channels[19]. The Brunauer-Emmett-Teller(BET) surface area (S_{BET}=694 m^2/g) as well as the mesoporous volume(V_{meso}=0.74 cm^3/g) of PHTS is less than those of SBA-15(Table 1). The Barrett-Joyner-Halenda(BJH) pore size(D_{BJH}) of PHTS is 7.1 nm, nearly equal to that of SBA-15, 7.2 nm[Fig.3(B) and Table 1], implying that plugging of hexagonal channels did not affect the pore size of the mesopores in PHTS.

Table 1 Pore parameters of SBA-15, PHTS and MIOs

Sample	S_{BET}/ ($m^2 \cdot g^{-1}$)	V_{meso}/ ($cm^3 \cdot g^{-1}$)	V_{micro}/ ($cm^3 \cdot g^{-1}$)	D_{BJH}/ nm
SBA-15	716	0.83	0.06	7.1
PHTS	694	0.74	0.09	7.2
MIO-500	82	0.26*	0.006	22.9
MIO-600	64	0.20*	0.003	89.2

* The value is composed of mesopore and macropore volumes.

Fig.4(A) shows the XRD patterns of MIO-500 and MIO-600. The single peak can be assigned to the (100) plane of the hexagonal framework negatively replicated from PHTS. The wide-angle XRD patterns[Fig.4(B)] suggest that the MIOs are hematite(α-Fe_2O_3, JCPDS-ICDD PDF No. 33-0664) in mineragraphy. The Bragg diffraction peaks of MIOs are sharp and narrow in our case, while the peaks of mesoporous α-Fe_2O_3 are low and broad with large diffuse-reflecting backgrounds[16], implying the higher crystallinity of MIOs as compared to that of the mesoporous α-Fe_2O_3 nanocasted from KIT-6.

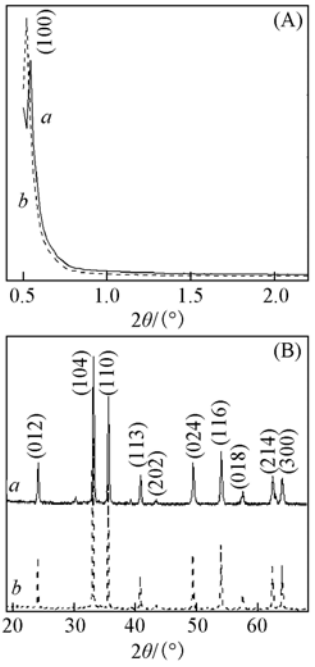

Fig.4 Small(A) and wide(B) angle XRD patterns of MIO-500(*a*) and MIO-600(*b*)

The N_2 adsorption-desorption isotherms of MIOs belong to type IV isotherm combined with type H2 conjunct and type H3 hysteresis loop[Fig.5(A)], suggesting the coexistence of wormhole-like mesopores and slit-like macropores in MIOs[21]. The BJH pore size distributions[Fig.5(B)] were centered around 22.9 and 89.2 nm for MIO-500 and MIO-600, respectively. The BET surface areas(S_{BET}) of MIO-500 and MIO-600 are 82 and 64 m^2/g, respectively(Table 1), less than that of mesoporous α-Fe_2O_3 nanocasted from KIT-6[16]. The decreasing BET surface area of MIOs may be probably resulted from the aggregation of iron oxide particles during the template-removing process. The mesoporous volumes(V_{meso}) of MIOs are 0.26 and 0.20 cm^3/g for MIO-500 and MIO-600, respectively. The microporous volumes(V_{micro}) are 0.006 and 0.003 cm^3/g for MIO-500 and MIO-600, respectively, considerably less than that of PHTS(Table 1).

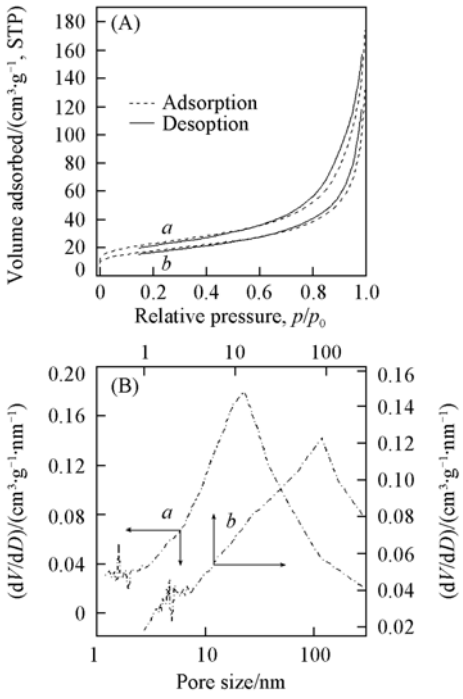

Fig.5 N_2 adsorption-desorption isotherms(A) and pore size distributions(B) of MIOS

a. MIO-500; *b*. MIO-600.

TEM images of MIO-500(Fig.6) show that there is a large amount of wormhole-like mesopores in addition to many well-defined micropore arrays[marked with parallel white lines, Fig.6(B)]. The mesopores are connected to form a wormhole-like network, well consistent with the N_2 adsorption data[Fig.5(A)]. Energy-dispersive X-ray(EDX) spectroscopic analysis[inset in Fig.6(A)] reconfirms that MIO-500 is hematite in mineragraphy. Moreover, the inset in Fig.6(B) illustrates clear lattice fringes with an interplanar spacing of 0.37 nm that is corresponding to the face spacing (012) of hematite. This result coincides well with the EDX[inset of Fig.6(A)] and XRD data[Fig.4(B)].

Fig.7 depicts the adsorption isotherms of MIO-500 and natural hematite(α-Fe_2O_3). Two adsorption algorithms, Langmuir and Freundlich, were used to describe the adsorption isotherms. Langmuir equation was employed to calculate the adsorption capacities—the theoretical maximum adsorption capacity(q_m). As to Langmuir algorithm, linear plots of C_e/q_e *versus* C_e[C_e is the equilibrium concentration of As(V), whereas q_e is the equilibrium adsorption capacity] for MIO-500 were achieved with regression coefficient(R^2), b(L/mg), and

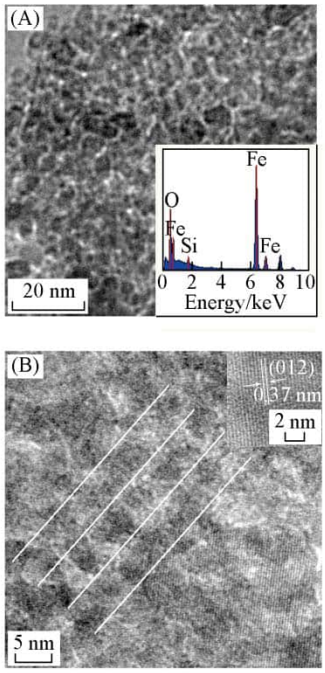

Fig.6 TEM images of MIO-500 with wormhole-like mesopores in low(A) and high(B) magnification

Inset of (A): EDX spectrum; inset of (B): lattice fringes of hematite.

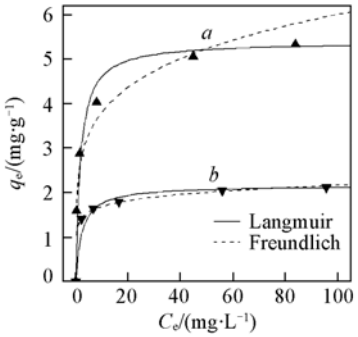

Fig.7 Adsorption isotherms of MIO-500(*a*) and *α*-Fe_2O_3(*b*)

q_m(mg/g) of 0.998, 0.13 and 5.39, respectively. For Freundlich algorithm, however, R^2 obtained by linear plotting of lnq_e *versus* lnC_e was 0.957, less than that achieved by Langmuir algorithm, suggesting that adsorption of As(V) onto MIO-500 follows the Langmuir isotherm model other than the Freundlich model. Likewise, the adsorption isotherm of natural hematite for As(V) is better fitted by Langmuir algorithm(R^2=0.994) than by Freundlich algorithm(R^2=0.978). The As(V) maximum adsorption capacity of natural hematite is 2.16 mg/g according to Langmuir algorithm. We noted that the maximum adsorption capacity of MIO-500(q_m=5.39 mg/g) is 2.5 times as large as that of the natural hematite adsorbent(q_m=2.16 mg/g). Nevertheless, the mechanism for As(V) adsorption on both the natural and synthetic hematite materials would be the same[22], namely, the surface complexation[23]. Hence, the reason accounting for the greater adsorption capacity of MIO-500 seems to arise from the larger BET surface area(82 m^2/g) as compared to that of the natural hematite adsorbent(*ca*. 12—18 m^2/g from the datasheet of the adsorbent). In summary, the adsorption results indicate that the nanocasted MIOs could be potentially used as adsorbent for As(V).

4 Conclusions

PHTS with a BET surface area of 694 m^2/g was facilely prepared with sodium silicate and P123 as the silica source and the structure-directing agent. With the synthetic PHTS as hard-template, MIOs were successfully prepared. The data obtained by XRD, TEM and N_2 adsorption-desorption suggest that MIO-500 with a BET surface area of 82 m^2/g is synthetic hematite with a wormhole-like mesoporous network. Comparison of As(V) adsorptions on selected MIO-500 and natural hematite was made. The result suggests that MIOs could be used as alternative candidates for adsorption of As(V) in wastewater.

References

[1] Yang P. D., Zhao D. Y., Margolese D. I., Chmelka B. F., Stucky G. D., *Nature*, **1998**, *396*, 152
[2] Schuth F., *Chem. Mater.*, **2001**, *13*, 3184
[3] Lee J., Christopher O. M., Warren S. C., Kamperman M., Di Salvo F. J., Wiesner U., *Nat. Mater.*, **2008**, *7*, 222
[4] Fang D. R., Ren W. Z., Liu Z. M., Xu X. F., Zhang H. M., Liao W. P., *Chem. Res. Chinese Universities*, **2010**, *26*(1), 105
[5] Guli M. N., Chen Y. N., Li X. T., *Chem. Res. Chinese Universities*, **2011**, *27*(3), 350
[6] Huo Q. S., Margolese D. I., Ciesla U., Feng P. Y., Gier T. E., Sieger P., Leon R., Petroff P. M., Schuth F., Stucky G. D., *Nature*, **1994**, *368*, 317
[7] Jiao F., Bruce P. G., *Angew. Chem. Int. Ed.*, **2004**, *43*, 5958
[8] Han L., Shan Z., Chen D. H., Yu X. J., Yang P. Y., Tu B., Zhao D. Y., *J. Colloid Interface Sci.*, **2008**, *318*, 315
[9] Li F. H., Fu H., Zhai J. P., Li Q., *Micro. Meso. Mater.*, **2009**, *123*, 177
[10] Kruk M., Jaroniec M., Ryoo R., Joo S. H., *J. Phys. Chem. B*, **2000**, *104*, 7960
[11] Joo S. H., Jun S., Ryoo R., *Micro. Meso. Mater.*, **2001**, *44/45*, 153
[12] Ryoo R., Joo S. H., Kruk M., Jaroniec M., *Adv. Mater.*, **2001**, *13*, 677
[13] Wang Y. Q., Yang C. M., Schmidt W., Spliethoff B., Bill E., Schuth F., *Adv. Mater.*, **2005**, *17*, 53
[14] Lu A. H., Schuth F., *Adv. Mater.*, **2006**, *18*, 1793
[15] Roggenbuck J., Schafer H., Tsoncheva T., Minchev C., Hanss J., Tiemann M., *Micro. Meso. Mater.*, **2007**, *101*, 335
[16] Jiao F., Harrison A., Jumas J. C., Chadwick A. V., Kockelmann W., Bruce P. G., *J. Am. Chem. Soc.*, **2006**, *128*, 5468
[17] Jiao F., Jumas J. C., Womes M., Chadwick A. V., Harrison A., Bruce P. G., *J. Am. Chem. Soc.*, **2006**, *128*, 12905
[18] Jiao F., Yue B., Zhu K. K., Zhao D. Y., He H. Y., *Chem. Lett.*, **2003**, *32*, 770
[19] van der Voort P., Ravikovitch P. I., de Jong K. P., Benjelloun M., van Bavel E., Janssen A. H., Neimark A. V., Weckhuysen B. M., Vansant E. F., *J. Phys. Chem. B*, **2002**, *106*, 5873
[20] Zhao D. Y., Huo Q. S., Feng J. L., Chmelka B. F., Stucky G. D., *J. Am. Chem. Soc.*, **1998**, *120*, 6024
[21] Kruk M., Jaroniec M., *Chem. Mater.*, **2001**, *13*, 3169
[22] Gimenez J., Martinez M., de Pablo J., Rovira M., Duro L., *J. Hazard. Mater.*, **2007**, *141*, 575
[23] Sherman D. M., Randall S. R., *Geochim. Cosmochim. Acta*, **2003**, *67*, 4223